

- (33) B. H. O'Conner and E. N. Maslen, *Acta Crystallogr.*, **20**, 824 (1966).
 (34) F. Hanic, *Acta Crystallogr.*, **17**, 633 (1964).
 (35) A. Bondi, *J. Phys. Chem.*, **68**, 441 (1964).
 (36) G. E. Bacon and N. A. Curry, *Proc. R. Soc. London, Ser. A*, **266**, 95 (1962).
 (37) E. Sletten and B. Thorstensen, *Acta Crystallogr., Sect. B*, **30**, 2438 (1974).
 (38) B. Bleaney and K. D. Bowers, *Proc. R. Soc. London, Ser. A*, **214**, 451 (1952).
 (39) A. R. Miedena, H. Van Kempen, T. Haseda, and W. J. Huiskamp, *Physica (Utrecht)*, **28**, 119 (1962).
 (40) S. Wittekoek, N. J. Poullis, and A. R. Miedena, *Physica (Utrecht)*, **30**, 1051 (1964).
 (41) T. P. Mitchell, W. H. Bernard, and J. R. Wasson, *Acta Crystallogr., Sect. B*, **26**, 2096 (1970).
 (42) B. J. Cole and W. H. Brumage, *J. Chem. Phys.*, **53**, 4718 (1970).
 (43) T. R. Felthouse, E. J. Laskowski, and D. N. Hendrickson, *J. Chem. Soc., Chem. Commun.*, 778 (1976).
 (44) J. A. Bertrand and F. T. Helm, *J. Am. Chem. Soc.*, **95**, 8184 (1973).
 (45) J. A. Bertrand, J. H. Smith, and P. G. Eller, *Inorg. Chem.*, **13**, 1649 (1974).
 (46) J. A. Bertrand, J. H. Smith, and D. G. VanDerveer, *Inorg. Chem.*, **16**, 1477 (1977).
 (47) J. J. Girerd, M. F. Charlot, and O. Kahn, *Mol. Phys.*, **34**, 1063 (1977).
 (48) Forticon 8, Quantum Chemistry Program Exchange, No. 344, Indiana University, Bloomington, Indiana.
 (49) G. Burns, *J. Chem. Phys.*, **41**, 1521 (1964).
 (50) J. W. Richardson, W. C. Nieuwpoort, R. R. Powell, and W. F. Edgell, *J. Chem. Phys.*, **36**, 1057 (1962).
 (51) O. Kahn and B. Briat, *J. Chem. Soc., Faraday Trans 2*, **72**, 1441 (1976).

Contribution from the Department of Chemistry, Simon Fraser University, Burnaby, British Columbia, V5A 1S6, Canada

Crystal Structure of Bis(ethanol)(octaethylporphinato)iron(III) Perchlorate-Ethanol

FREDERICK W. B. EINSTEIN* and ANTHONY C. WILLIS

Received April 18, 1978

The crystal structure of the title compound was determined using 2095 reflections (1822 with $I > 2.3\sigma_I$ used in refinement) measured on a four-circle automated diffractometer using monochromatic Mo $K\alpha_1$ radiation. The complex crystallized in the monoclinic space group $P2_1$: $a = 11.739$ (4) Å, $b = 18.158$ (7) Å, $c = 10.062$ (3) Å, $\beta = 90.45$ (2)°. The final value for the discrepancy index was $R_1 = 0.055$. The iron atom lies in the plane of the porphine coordinated to the four nitrogen atoms (Fe-N = 2.026 (9)–2.042 (8) Å) and, axially, to the oxygen atoms of two ethanol molecules (Fe-O = 2.113 (8), 2.160 (8) Å). Both the equatorial and axial bonds are considerably longer than those of low-spin porphinatoiron(III) complexes, consistent with a mixed- or high-spin electronic ground state.

In recent years several porphinato iron complexes have been prepared which have intermediate-spin ground states.^{1,2} In particular (octaethylporphinato)iron(III) perchlorate (Fe(OEP)ClO₄) and Fe(OEP)ClO₄·2EtOH have ground states with $S = 3/2$ which have been shown to be single-spin states and not thermally induced spin crossovers. These two compounds were thought to be structurally quite different as there was evidence of iron-perchlorate interactions in Fe(OEP)ClO₄ and of iron-ethanol interactions in Fe(OEP)ClO₄·2EtOH. It was predicted that the former would have a coordination number of 5 and the latter 6.¹

This study was initiated to determine the stereochemistry of the solvated species. The geometry about the iron atom was expected to resemble that of low-spin porphinatoiron(III) complexes, but with some small differences in bond lengths owing to changes in the occupancy of some of the d orbitals.

Experimental Section

Fe(OEP)ClO₄·2EtOH was prepared by the standard method.¹ Crystals were obtained by the slow evaporation of an ethanol solution of the complex, but if left to stand in the air for any length of time the crystals lost solvent and became unsuitable for X-ray crystallographic studies. To prevent efflorescence, a large crystal was freshly prepared and a prismatic fragment of axial dimensions 0.80 × 0.50 × 0.50 mm cleaved off, immediately covered in grease and sealed in a Lindemann tube. Photographs taken of the crystal fragment with Cu $K\alpha$ radiation revealed Laue $2/m$ symmetry and gave approximate unit cell parameters. They also confirmed that the crystal was not decomposing. Accurate cell dimensions were obtained by a least-squares analysis from the setting angles of nine reflections with $2\theta > 25^\circ$ which were accurately centered on a Picker FACS-I four-circle automated diffractometer employing monochromatic Mo $K\alpha_1$ radiation. Crystal data are given in Table I. The intensities of 2095 unique reflections with $2\theta < 40^\circ$ were measured and of these 1822 with $I > 2.3\sigma_I$ (σ_I is the standard deviation in the intensity derived from counter statistics) were regarded as observed and used in structure solution and refinement. The average intensity of reflections decreased rapidly with increasing 2θ so data were collected in two shells (see Table II). Two standard reflections were measured after every 75

Table I. Crystal Data

C ₄₂ H ₆₂ ClFeN ₄ O ₇	fw 826.29
space group $P2_1$	$\mu = 4.79 \text{ cm}^{-1}$
$a = 11.739$ (4) Å	$\rho_o^a = 1.27 \text{ g cm}^{-3}$
$b = 18.158$ (7) Å	$\rho_c = 1.279 \text{ g cm}^{-3}$
$c = 10.062$ (3) Å	final $R_1^b = 0.055$
$\beta = 90.45$ (2)°	final $R_2^c = 0.061$
$U = 2144.7 \text{ Å}^3$	final extinction
$Z = 2$	correction 2.2 (4) × 10 ⁻⁵

^a Flotation in C₆H₆/CCl₄. ^b $R_1 = \sum ||F_o| - |F_c|| / \sum |F_o|$. ^c $R_2 = (\sum w(|F_o| - |F_c|)^2 / \sum |F_o|^2)^{1/2}$.

Table II. Data Collection

radiation	monochromatic Mo $K\alpha_1$ (λ 0.709 26 Å)
takeoff angle	5°
θ - 2θ scan	2° min ⁻¹
scan width with	$2\theta \leq 30^\circ$, $(1.2 + 0.692 \tan \theta)^\circ$;
dispersion cor	$30^\circ < 2\theta \leq 40^\circ$, $(1.1 + 0.692 \tan \theta)^\circ$
stationary-crystal,	$2\theta \leq 30^\circ$, 4 s at each scan limit;
stationary-counter	$30^\circ < 2\theta \leq 40^\circ$, 10 s at each scan limit
bgd counts	

data points and the data scaled accordingly. No absorption correction was applied.

Solution and Refinement of the Structure

The structure was solved by conventional heavy-atom procedures. Least-squares refinement of the nonhydrogen atoms with individual isotropic temperature factors yielded $R_1 = 0.101$. The coordinates of the hydrogen atoms attached to nonmethyl carbons were determined geometrically (sp^2 or sp^3 coordination at the carbon, $r_{C-H} = 0.95$ Å). The H($n1$) atoms were assigned the average temperature factor of the C($n1$) atoms and the H($n3A$) and H($n4A$) the average of the eight C($n3A$) and C($n4A$). These hydrogen atom parameters were not refined, but the scattering contribution was included in all further calculations. In addition, the iron atom and the atoms of the perchlorate were assigned anisotropic temperature factors, the resultant R_1 being 0.072. A difference map using data $2\theta < 32^\circ$ revealed H(5), H(7), and many of the methyl hydrogen atoms. The remaining hydrogens were positioned geometrically from these. Examination

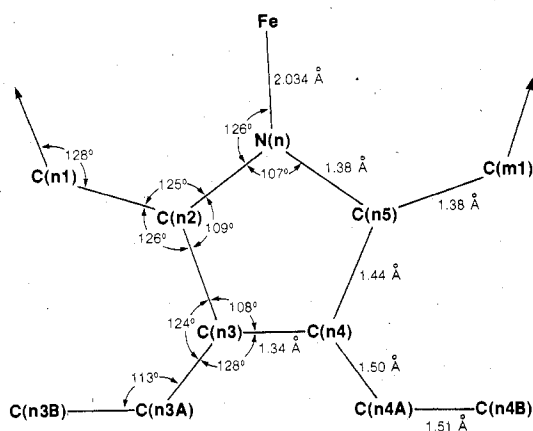


Figure 1. Atom-labeling scheme for the pyrrole rings and averaged geometry.

of a full-data difference map indicated that C(14B), C(34B), and O(7) should also be anisotropic and that the ethanol carbon atoms were disordered. Each ethanol carbon atom was therefore assigned two sites with estimated relative occupancies which were adjusted during further refinement to give equal temperature factors for both sites. Resolution was achieved for all but C(7B) which was therefore considered to be one site with strongly anisotropic thermal motion. This model for the ethanol molecules is not ideal but adequate: any shortcomings will have little effect on the geometry of the iron coordination sphere and the porphine core. The only major feature in a final difference map was a peak of $0.27 \text{ e } \text{Å}^{-3}$ ($\sigma_p = 0.06 \text{ e } \text{Å}^{-3}$) at (0.198, 0.059, 0.561) within the perchlorate group. Attempts to fit this peak by adjustment of the perchlorate geometry were unsuccessful and refinement was terminated at this point. The function being minimized in the least-squares analysis was $\sum w(|F_o| - |F_c|)^2 / (1 + E_c I)$. In early stages of refinement unit weights were used ($w = 1$) and the isotropic extinction parameter was set to zero ($E_c = 0$); in the final cycles the weighting scheme was of the form $w = 1/\sigma_p^2$ and E_c was refined. All shift-to-error ratios in the final cycle were less than 0.1. Neutral scattering factors³ were employed and anomalous dispersion corrections⁴ applied for Fe and Cl. A description of the computer programs has been given previously.⁵

The atomic coordinates and associated thermal parameters are listed in Table III, bond lengths and angles in Table IV, and relevant least-squares planes in Table V. Figure 1 shows the numbering scheme of the porphyrin and the averaged geometry assuming that the halves of all of the pyrrole rings are equivalent.

Description and Discussion

The crystal structure consists of discrete $[\text{Fe}(\text{OEP})(\text{EtOH})_2]^+$ cations, perchlorate anions, and ethanol molecules of crystallization giving an overall stoichiometry of $\text{Fe}(\text{OEP})\text{ClO}_4 \cdot 3\text{EtOH}$ rather than $\text{Fe}(\text{OEP})\text{ClO}_4 \cdot 2\text{EtOH}$ as previously reported by Dolphin.¹ There is considerable doubt that the structure reported here is of Dolphin's compound (see below).

The OEP macrocycle has approximate C_{2h} symmetry (see Figure 2 for a stereoscopic view of the cation). Several of the individual values differ from the mean by significant amounts, but in view of their apparent chemical equivalence they appear

simply to be aberrations. There is no indication of D_{2d} ruffling of the porphine core; the deviations of the methine carbons from the least-squares plane of the core are all $< 0.03 \text{ Å}$ and do not have the correct signs for the "circular standing wave" configuration.⁶

The terminal ethyl carbon atoms assume a $++$, $++$, $--$, $--$ conformation⁷ as in uncoordinated $\text{H}_2(\text{OEP})$.⁸ Examples of four-, five-, and six-coordinate metalloporphyrins with this conformation are known.⁹ Other conformations have also been reported.¹⁰

The iron atom lies approximately in the plane of the OEP macrocycle and is coordinated to the four porphine nitrogens. The oxygen atoms of two ethanol molecules complete an approximately octahedral coordination geometry around the iron atom. There is no evidence of doming for, although the iron atom is displaced axially from the center of the nitrogen atoms by 0.008 Å , the nitrogen atoms themselves are not coplanar and deviate from the least-squares "plane" they define by comparable distances.

The $\text{Fe}-\text{N}_{\text{porph}}$ bond lengths (2.026 (9), 2.029 (8), 2.040 (7), and 2.042 (8) Å) are considerably longer than those of the low-spin six-coordinate complexes $[\text{Fe}(\text{TPP})(\text{Im})_2]^+$ (TPP = 5,10,15,20-tetraphenylporphine, Im = imidazole) (1.980–1.999 Å)¹¹ and $[\text{Fe}(\text{PP-IX})(1\text{-Me-Im})_2]^+$ (PP-IX = protoporphyrin IX) (1.973–2.012 Å),¹² but are comparable with those of two other mixed- or high-spin six-coordinate porphyratoiron(III) complexes, $[\text{Fe}(\text{TPP})(\text{H}_2\text{O})_2]^+$ (2.035–2.041 Å) and $[\text{Fe}(\text{TPP})(\text{TMSO})_2]^+$ (TMSO = tetramethylene sulfoxide) (average 2.045 (5) Å).² In five-coordinate high-spin Fe(III) complexes the $\text{Fe}-\text{N}_{\text{porph}}$ bonds are typically 2.065 Å with a very short Fe-axial atom distance.⁶

As the oxygen atoms of the coordinated ethanol molecules did not require a disordered-atom description, the difference between the two Fe-O bond lengths (2.112 (8); cf. 2.160 (8) Å) is apparently significant. A smaller, but also meaningful, asymmetry is reported for $[\text{Fe}(\text{TPP})(\text{TMSO})_2]^+$ (2.087 (3) Å; cf. 2.069 (3) Å), but in $[\text{Fe}(\text{TPP})(\text{H}_2\text{O})_2]^+$ the axial bonds are crystallographically constrained to be equal (2.090 (2) Å). Asymmetry of the axial bonds is also observed in $[\text{Fe}(\text{TPP})(\text{Im})_2]$ and $[\text{Fe}(\text{PP-IX})(1\text{-Me-Im})_2]^+$ where it was accredited to a nonbonding interaction between the imidazole 2,4 hydrogen atoms and the porphine nitrogens.^{11,12} The interaction will be a maximum when the dihedral angle between the $\text{Fe}-\text{N}_{\text{Im}}-\text{N}_{\text{porph}}$ plane and the imidazole plane verges on 0 or 90° causing the $\text{Fe}-\text{N}_{\text{Im}}$ bond to lengthen concomitantly. A corresponding relationship may exist for $[\text{Fe}(\text{OEP})(\text{EtOH})_2]^+$ but cannot be satisfactorily tested as the ethanol carbon atoms are disordered and therefore the hydrogen atom positions are very poorly defined. It would seem likely, however, that the greater geometric freedom of the ethanol molecules could reduce the importance of the effect. The iron atom is displaced from the least-squares plane through the porphine nitrogens in the direction of the *closer* oxygen atom in contrast to the imidazole derivatives where the displacement of $\sim 0.009 \text{ Å}$ is toward the *more distant* axial atom.

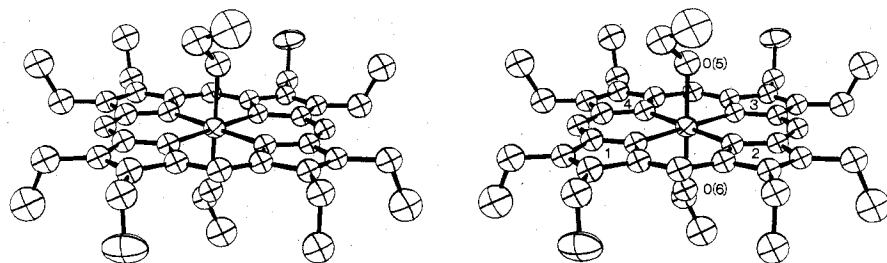


Figure 2. Stereoscopic view of the molecule showing ring numbering. Here and in Figure 3 the thermal ellipsoids show 50% probability levels, and the hydrogen atoms and the minor orientations of the disordered molecules have been deleted for clarity.

Table III. Final Positional and Thermal Parameters for $[\text{Fe}(\text{OEP})(\text{C}_2\text{H}_5\text{OH})_2]^+\text{ClO}_4^-\cdot\text{C}_2\text{H}_5\text{OH}^a$

(a) Nonhydrogen Atoms ^b									
atom	x	y	z	$U, \text{\AA}^2$	atom	x	y	z	$U, \text{\AA}^2$
Fe	5667 (1)	2500 (-)	6806 (2)		C(12)	3374 (9)	2954 (6)	7924 (10)	50 (3)
N(3)	6957 (6)	2391 (5)	5474 (7)	42 (2)	C(13)	2677 (9)	2878 (6)	9079 (11)	51 (3)
C(31)	8279 (9)	1676 (6)	6830 (10)	45 (3)	C(13A)	1492 (10)	3197 (7)	9230 (11)	70 (4)
C(32)	7969 (8)	2028 (6)	5682 (10)	43 (3)	C(13B)	0586 (12)	2658 (9)	8789 (14)	106 (5)
C(33)	8610 (9)	2064 (6)	4452 (10)	50 (3)	C(14)	3246 (9)	2480 (9)	9989 (10)	60 (3)
C(33A)	9755 (11)	1718 (7)	4275 (12)	69 (4)	C(14A)	2887 (11)	2212 (7)	11312 (12)	74 (4)
C(33B)	10743 (12)	2204 (8)	4611 (13)	90 (4)	C(14B)	2424 (14)	1443 (9)	11303 (13)	
C(34)	4764 (8)	2467 (7)	3587 (9)	47 (3)	C(15)	4357 (9)	2284 (6)	9377 (10)	52 (3)
C(34A)	8386 (9)	2692 (6)	2215 (10)	60 (3)	N(2)	6586 (7)	1900 (5)	8155 (8)	46 (2)
C(34B)	8985 (12)	3423 (7)	2138 (13)		C(21)	5213 (9)	1890 (6)	9967 (11)	54 (3)
C(35)	6988 (8)	2679 (6)	4187 (9)	47 (3)	C(22)	6237 (9)	1709 (6)	9416 (10)	50 (3)
N(4)	4761 (7)	3098 (5)	5467 (8)	48 (2)	C(23)	7146 (9)	1293 (6)	10049 (10)	48 (3)
C(41)	6116 (9)	3096 (6)	3620 (10)	49 (3)	C(23A)	7064 (10)	972 (7)	11424 (12)	63 (3)
C(42)	5086 (9)	3291 (6)	4170 (10)	52 (3)	C(23B)	6460 (11)	225 (7)	11463 (12)	78 (4)
C(43)	4178 (10)	3696 (6)	3537 (11)	55 (3)	C(24)	7977 (9)	1245 (6)	9184 (10)	46 (3)
C(43A)	4210 (11)	4001 (8)	2146 (12)	70 (4)	C(24A)	9112 (10)	869 (7)	9431 (11)	61 (4)
C(43B)	4595 (12)	4791 (9)	2116 (13)	95 (5)	C(24B)	9051 (13)	54 (9)	9079 (15)	100 (5)
C(44)	3319 (9)	3748 (6)	4430 (10)	54 (3)	C(25)	7636 (8)	1605 (6)	7990 (9)	43 (3)
C(44A)	2175 (12)	4099 (7)	4234 (13)	75 (4)	Cl	2110 (3)	581 (2)	7140 (4)	
C(44B)	2105 (13)	4887 (9)	4725 (14)	94 (5)	O(1)	2734 (11)	1222 (7)	7083 (15)	
C(45)	3678 (9)	3371 (6)	5618 (10)	53 (3)	O(2)	985 (9)	688 (9)	6686 (13)	
N(1)	4374 (7)	2589 (6)	8122 (8)	49 (2)	O(3)	2642 (10)	12 (7)	6489 (13)	
C(11)	3070 (9)	3315 (6)	6760 (10)	50 (3)	O(4)	2040 (12)	347 (9)	8461 (13)	

atom	occu- pancy	x	y	z	$U, \text{\AA}^2$	atom	occu- pancy	x	y	z	$U, \text{\AA}^2$
O(5)	1.00	6438 (6)	3482 (4)	7490 (7)	63 (2)	C(6A)P	0.50	5073 (24)	1090 (17)	5000 (29)	73 (8)
C(5A)	0.65	6150 (20)	3962 (15)	8640 (22)	84 (7)	C(6B)	0.61	4634 (23)	635 (18)	4276 (26)	104 (8)
C(5A)P	0.35	6806 (41)	3627 (26)	9012 (49)	80 (13)	C(6B)P	0.39	4132 (37)	1265 (28)	4042 (45)	102 (15)
C(5B)	0.49	6990 (44)	3869 (35)	9644 (51)	150 (20)	O(7)	1.00	7791 (10)	4269 (6)	5943 (9)	
C(5B)P	0.51	6725 (37)	4418 (37)	9328 (44)	145 (16)	C(7A)	0.82	8978 (20)	4192 (13)	6076 (20)	108 (7)
O(6)	1.00	4860 (6)	1505 (4)	6093 (7)	60 (2)	C(7A)P	0.18	8822 (88)	4827 (62)	6512 (9)	108 (31)
C(6A)	0.50	4616 (28)	1405 (17)	4669 (31)	72 (8)	C(7B)	1.00	9497 (17)	4637 (17)	7039 (22)	

atom	U_{11}^c	U_{22}	U_{33}	U_{12}	U_{13}	U_{23}	atom	U_{11}	U_{22}	U_{33}	U_{12}	U_{13}	U_{23}
Fe	47 (1)	48 (1)	36 (1)	-2 (1)	10 (1)	5 (1)	O(2)	90 (9)	233 (15)	194 (12)	34 (10)	-12 (8)	78 (12)
C(14B)	156 (15)	96 (12)	72 (9)	-39 (11)	44 (9)	8 (9)	O(3)	111 (9)	139 (10)	198 (12)	15 (8)	9 (8)	-82 (10)
C(34B)	112 (11)	63 (9)	73 (9)	-24 (8)	34 (8)	5 (7)	O(4)	177 (13)	236 (18)	121 (10)	2 (12)	-12 (9)	33 (11)
Cl	63 (2)	78 (3)	103 (3)	-2 (2)	15 (2)	-16 (2)	O(7)	116 (9)	144 (10)	103 (7)	-45 (7)	-15 (6)	58 (7)
O(1)	155 (11)	87 (8)	261 (16)	-53 (8)	92 (11)	-36 (9)	C(7B)	96 (15)	266 (33)	182 (21)	8 (19)	-44 (15)	-32 (22)

(b) Hydrogen Atoms ^d							
atom	x	y	z	atom	x	y	z
H(11)	233	356	676	H(31)	904	145	684
H1(13A)	143	364	869	H1(33A)	982	157	334
H2(13A)	137	332	1017	H2(33A)	979	128	484
H1(13B)	60	264	776	H1(33B)	1092	251	372
H2(13B)	46	229	933	H2(33B)	1144	196	481
H3(13B)	-15	292	877	H2(33B)	1054	258	523
H1(14A)	230	254	1165	H1(34A)	771	272	165
H2(14A)	355	223	1191	H2(34A)	890	231	188
H1(14B)	306	105	1167	H1(34B)	962	345	280
H2(14B)	226	122	1041	H2(34B)	846	383	231
H3(14B)	179	133	1188	H3(34B)	934	351	124
H(21)	508	172	1088	H(41)	625	328	272
H1(23A)	664	132	1198	H1(43A)	344	397	176
H2(23A)	783	91	1179	H2(43A)	474	370	162
H1(23B)	660	-6	1233	H1(43B)	429	508	289
H2(23B)	662	-11	1074	H2(43B)	431	503	130
H3(23B)	557	28	1146	H3(43B)	544	485	214
H1(24A)	932	92	1037	H1(44A)	161	381	471
H2(24A)	969	110	888	H2(44A)	199	410	328
H1(24B)	882	-9	825	H1(44B)	230	489	577
H2(24B)	869	-24	991	H2(44B)	130	509	483
H3(24B)	981	-21	919	H3(44B)	257	524	433
H(5)	707	374	701	H1(6A)P	509	53	529
H1(5A)	540	383	894	H2(6A)P	589	117	471
H2(5A)	615	447	829	H(7)	748	442	518
H1(5A)P	759	344	909	H1(7A)	932	433	522
H2(5A)P	631	331	955	H2(7A)	916	368	627
H1(6A)	526	161	417	H1(7A)P	848	523	703
H2(6A)	392	157	443	H2(7A)P	919	507	571

^a Estimated standard deviations of the least significant figures are given in parentheses here and in succeeding tables. ^b The values of the positional parameters are multiplied by 10^4 and thermal parameters (in \AA^2) by 10^3 . ^c Anisotropic temperature factors are in the form $\exp[-2\pi^2(U_{11}h^2a^{*2} + \dots + 2U_{23}kib^*c^*)]$. ^d The values of the positional parameters are multiplied by 10^3 .

Table IV. Interatomic Distance (Å) and Angles (deg)

a. Coordination Sphere				
Fe-N(1)	2.029 (8)	Fe-N(4)	2.026 (9)	
Fe-N(2)	2.042 (8)	Fe-O(5)	2.113 (8)	
Fe-N(3)	2.040 (7)	Fe-O(6)	2.160 (8)	
N(1)-Fe-N(2)	90.2 (3)	N(2)-Fe-O(6)	90.2 (3)	
N(1)-Fe-N(3)	178.9 (5)	N(3)-Fe-N(4)	90.2 (3)	
N(1)-Fe-N(4)	89.9 (3)	N(3)-Fe-O(5)	88.8 (3)	
N(1)-Fe-O(5)	92.3 (4)	N(3)-Fe-O(6)	91.5 (3)	
N(1)-Fe-O(6)	87.4 (3)	N(4)-Fe-O(5)	89.2 (3)	
N(2)-Fe-N(3)	89.7 (3)	N(4)-Fe-O(6)	90.0 (3)	
N(2)-Fe-N(4)	179.8 (4)	O(5)-Fe-O(6)	179.2 (3)	
N(2)-Fe-O(5)	90.6 (3)			
b. Porphyrin ^a				
	<i>n</i> = 1	<i>n</i> = 2	<i>n</i> = 3	<i>n</i> = 4
{ C(n1)-C(n2)	1.39 (1)	1.37 (1)	1.37 (1)	1.38 (1)
{ C(n5)-C(m1)	1.36 (1)	1.40 (1)	1.39 (1)	1.36 (1)
{ N(n)-C(n2)	1.35 (1)	1.38 (1)	1.37 (1)	1.41 (1)
{ N(n)-C(n5)	1.38 (1)	1.36 (1)	1.40 (1)	1.37 (1)
{ C(n2)-C(n3)	1.43 (1)	1.45 (1)	1.45 (1)	1.44 (1)
{ C(n5)-C(n4)	1.49 (1)	1.42 (1)	1.42 (1)	1.44 (1)
{ C(n3)-C(n4)	1.34 (2)	1.32 (1)	1.33 (1)	1.36 (1)
{ C(n3)-C(n3A)	1.52 (2)	1.51 (2)	1.50 (2)	1.50 (2)
{ C(n4)-C(n4A)	1.48 (2)	1.52 (1)	1.50 (1)	1.50 (2)
{ C(n3A)-C(n3B)	1.51 (2)	1.53 (2)	1.49 (2)	1.51 (2)
{ C(n4A)-C(n4B)	1.50 (2)	1.52 (2)	1.50 (2)	1.51 (2)
{ C(p5)-C(n1)-C(n2)	128.0 (11)	126.6 (11)	127.3 (10)	128.2 (10)
{ C(n1)-C(n2)-N(n)	124.7 (10)	125.4 (10)	125.3 (9)	123.6 (10)
{ C(m1)-C(n5)-N(n)	126.3 (10)	124.2 (9)	124.0 (9)	123.9 (10)
{ C(n1)-C(n2)-C(n3)	125.9 (10)	126.4 (10)	127.2 (9)	127.0 (10)
{ C(m1)-C(n5)-C(n4)	126.1 (10)	126.6 (9)	127.2 (9)	125.9 (10)
{ N(n)-C(n2)-C(n3)	109.4 (9)	108.1 (9)	107.5 (8)	109.4 (9)
{ N(n)-C(n5)-C(n4)	107.5 (9)	109.2 (9)	108.8 (8)	110.2 (9)
{ C(n2)-N(n)-C(n5)	108.1 (8)	106.9 (9)	107.0 (7)	105.7 (9)
{ C(n2)-N(n)-Fe	126.3 (7)	125.9 (7)	126.3 (6)	127.2 (7)
{ C(n5)-N(n)-Fe	125.5 (7)	127.3 (7)	126.7 (6)	127.0 (7)
{ C(n2)-C(n3)-C(n4)	108.7 (10)	106.9 (9)	108.3 (9)	107.1 (10)
{ C(n5)-C(n4)-C(n3)	106.3 (9)	108.9 (9)	108.2 (9)	107.6 (10)
{ C(n2)-C(n3)-C(n3A)	125.1 (10)	123.5 (10)	123.6 (10)	125.2 (10)
{ C(n5)-C(n4)-C(n4A)	123.3 (11)	125.9 (9)	124.6 (9)	124.6 (10)
{ C(n4)-C(n3)-C(n3A)	126.2 (10)	129.5 (10)	128.0 (10)	127.8 (11)
{ C(n3)-C(n4)-C(n4A)	130.3 (11)	125.2 (10)	127.1 (9)	127.7 (11)
{ C(n3)-C(n3A)-C(n3B)	111.5 (11)	113.6 (10)	115.0 (11)	112.3 (11)
{ C(n4)-C(n4A)-C(n4B)	113.9 (11)	111.1 (11)	115.0 (10)	114.2 (12)
c. Perchlorate				
Cl-O(1)	1.38 (1), 1.48 (1) ^b	Cl-O(3)	1.38 (1), 1.45 (1) ^b	
Cl-O(2)	1.41 (1), 1.50 (1) ^b	Cl-O(4)	1.40 (1), 1.50 (1) ^b	
O(1)-Cl-O(2)	111.5 (9)	O(2)-Cl-O(3)	112.2 (9)	
O(1)-Cl-O(3)	111.9 (7)	O(2)-Cl-O(4)	106.7 (8)	
O(1)-Cl-O(4)	109.4 (9)	O(3)-Cl-O(4)	104.7 (9)	
d. Ethanol				
O(5)-H(5)	1.00	C(6A)-C(6B)	1.45 (4)	
O(5)-C(5A)	1.49 (2)	C(6A)P-C(6B)P	1.49 (5)	
O(5)-C(5A)P	1.61 (5)	O(7)-H(7)	0.89	
C(5A)-C(5B)	1.42 (5)	O(7)-C(7A)	1.41 (2)	
C(5A)P-C(5B)P	1.48 (7)	O(7)-C(7A)P	1.68 (11)	
O(6)-C(6A)	1.47 (3)	C(7A)-C(7B)	1.40 (3)	
O(6)-C(6A)P	1.36 (3)	C(7A)P-C(7B)P	1.01 (10)	
Fe-O(5)-H(5)	123	Fe-O(6)-C(6A)	121 (1)	
Fe-O(5)-C(5A)	130 (1)	Fe-O(6)-C(6A)P	131 (1)	
Fe-O(5)-C(5A)P	124 (2)	O(6)-C(6A)-C(6B)	112 (4)	
H(5)-O(5)-C(5A)	106	O(6)-C(6A)P-C(6B)P	105 (3)	
H(5)-O(5)-C(5A)P	101	H(7)-O(7)-C(7A)	121	
O(5)-C(5A)-C(5B)	109 (3)	H(7)-O(7)-C(7A)P	114	
O(5)-C(5A)P-C(5B)P	110 (4)	O(7)-C(7A)-C(7B)	116 (2)	
		O(7)-C(7A)P-C(7B)	122 (10)	
e. Intermolecular Contacts ≤ 2.8 Å				
O(2)...H(31) ^c	2.68	O(3)...H3(43B) ^d	2.65	
O(2)...H2(24A) ^c	2.80	O(3)...H(7) ^d	2.00	
O(2)...H2(33A) ^c	2.55	O(4)...H2(14B)	2.53	
O(3)...H2(34B) ^d	2.79	O(7)...H(5)	1.68	

^a $m = n + 1$ except $n = 4$ when $m = 1$; $p = n - 1$ except $n = 1$ when $p = 4$. ^b Corrected for thermal motion. ^c Atom at $x - 1, y, z$. ^d Atom at $1 - x, y - 1/2, 1 - z$.

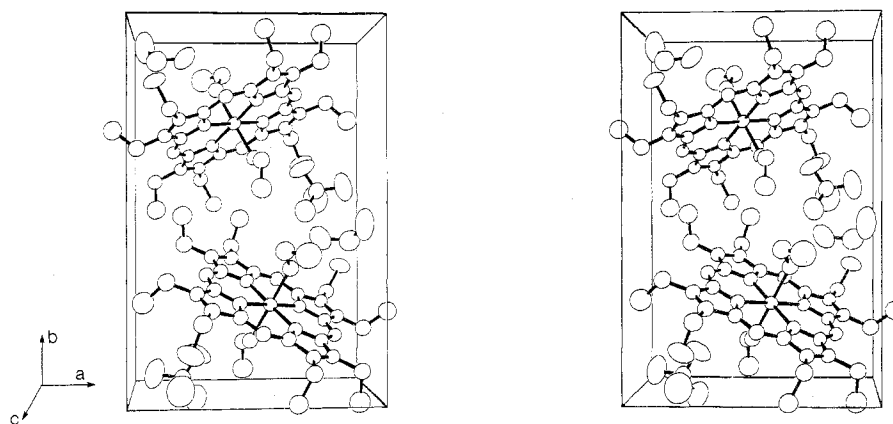


Figure 3. Molecular packing in the unit cell.

Table V

Least-Squares Planes ^a				
a. Plane through N(1), N(2), N(3), and N(4)				
$-0.4098x - 0.8406y - 0.3542z + 8.9380 = 0$ ($\chi^2 = 6.79$)				
N(1)	0.014	N(4)	-0.012	C(21) ^b 0.026
N(2)	-0.011	Fe ^b	-0.008	C(31) ^b -0.014
N(3)	0.010	C(11) ^b	0.015	C(41) ^b -0.009
b. Plane through N(1), N(3), O(5), and O(6)				
$-0.5206x + 0.5295y - 0.6698z + 5.6113 = 0$ ($\chi^2 = 5.07$)				
N(1)	-0.012	O(5)	0.008	Fe ^b -0.007
N(3)	-0.008	O(6)	0.007	
c. Plane through N(2), N(4), O(5), and O(6)				
$0.7346x - 0.1150y - 0.6687z + 0.2555 = 0$ ($\chi^2 = 0.74$)				
N(2)	0.004	O(5)	-0.003	Fe ^b 0.002
N(4)	0.004	O(6)	-0.003	
d. Plane through N(1), C(12), C(13), C(14), and C(15)				
$-0.4017x - 0.8343y - 0.3775z + 9.0459 = 0$ ($\chi^2 = 0.40$)				
N(1)	0.002	C(15)	0.000	C(14A) ^b 0.073
C(12)	-0.004	C(11) ^b	0.030	C(21) ^b -0.030
C(13)	0.004	C(13A) ^b	0.022	Fe ^b 0.022
C(14)	-0.004			
e. Plane through N(2), C(22), C(23), C(24), and C(25)				
$-0.3979x - 0.8477y - 0.3508z + 8.8452 = 0$ ($\chi^2 = 4.42$)				
N(2)	-0.009	C(25)	0.014	C(24A) ^b -0.047
C(22)	0.008	C(21) ^b	0.015	C(31) ^b 0.010
C(23)	0.002	C(23A) ^b	0.054	Fe ^b -0.031
C(24)	-0.010			
f. Plane through N(3), C(32), C(33), C(34), and C(35)				
$-0.4298x - 0.8364y - 0.3401z + 9.0054 = 0$ ($\chi^2 = 8.95$)				
N(3)	0.010	C(35)	-0.007	C(34A) ^b -0.065
C(32)	-0.020	C(31) ^b	-0.031	C(41) ^b -0.009
C(33)	0.018	C(33A) ^b	0.026	Fe ^b 0.043
C(34)	-0.006			
g. Plane through N(4), C(42), C(43), C(44), and C(45)				
$-0.3827x - 0.8555y - 0.3487z + 8.8498 = 0$ ($\chi^2 = 0.69$)				
N(4)	-0.003	C(45)	0.006	C(44A) ^b 0.031
C(42)	0.002	C(41) ^b	0.033	C(11) ^b -0.030
C(43)	0.001	C(43A) ^b	-0.003	Fe ^b 0.053
C(44)	-0.005			
Dihedral Angles between Planes (deg)				
a-d	1.46	d-e	1.73	a-b 89.68
a-e	0.82	e-f	2.04	a-c 88.14
a-f	1.42	f-g	2.96	b-c 89.74
a-g	1.80	g-d	2.32	

^a Deviations of atoms from the planes are given in Å. The equations of the planes are referred to the orthogonal axes *a*, *b*, and *c*. ^b Not used in defining plane.

For an iron(III) complex to have a purely $S = 3/2$ ground state the d_{z^2} and t_{2g} orbitals must be occupied while the $d_{x^2-y^2}$ orbital remains vacant. Structurally this will cause the axial bonds to be longer than in low-spin complexes but the equatorial bond lengths will stay similar. In [Fe(OEP)-

(EtOH)₂]⁺ the Fe-O distances are long, but the Fe-N distances are also long indicating that the $d_{x^2-y^2}$ orbital has an appreciable electron population. Consequently this complex does not have a pure $S = 3/2$ ground state but has either a quantum mechanical mixing of $S = 3/2$ and $5/2$ or simply high-spin $S = 5/2$. Dolphin's studies were carried out on a dried sample of this compound¹³ which analyzed for only two ethanol molecules. X-ray powder photographs show that a phase change occurs when triethanol crystals are dried, but it is not known if the iron environment of this compound differs from that of Dolphin's compound. The crystals effloresced too readily to allow the magnetic susceptibility or Mössbauer spectrum to be measured which would have clarified this point.

Hydrogen bonding plays an important role in the crystal packing as it connects all the molecular species. A list of the shorter hydrogen-heavy atom contacts is given in Table IV. There are three short O...O distances: O(3)...O(7), 2.84 (1); O(5)...O(7), 2.65 (1); O(1)...O(6), 2.74 (1) Å. The first is associated with the very short hydrogen bond O(3)...H(7)-O(7) and the second with O(7)...H(5)-O(5). The third is consistent with a hydrogen bond involving H(6), though that atom was not found in difference maps.

Acknowledgment. We are grateful for the financial support of the National Research Council of Canada which made this work possible. We also thank Drs. D. Dolphin and J. R. Sams (University of British Columbia) for the sample of Fe(OEP)ClO₄·2EtOH and for most helpful discussions and encouragement.

Registry No. Fe(OEP)ClO₄·2EtOH, 60645-79-6.

Supplementary Material Available: A listing of structure factor amplitudes (20 pages). Ordering information is given on any current masthead page.

References and Notes

- (1) D. H. Dolphin, J. R. Sams, and T. B. Tsin, *Inorg. Chem.*, **16**, 711 (1977).
- (2) M. E. Kastner, W. R. Scheidt, T. Mashiko, and C. A. Reed, *J. Am. Chem. Soc.*, **100**, 666 (1978).
- (3) Atomic scattering factors for hydrogen are from R. F. Stewart, E. R. Davidson, and W. T. Simpson, *J. Chem. Phys.*, **42**, 3175 (1965); others are from "International Tables for X-Ray Crystallography", Vol. IV, Kynoch Press, Birmingham, England, 1974, Table 2.2A.
- (4) D. T. Cromer and D. Liberman, *J. Chem. Phys.*, **53**, 1891 (1970).
- (5) F. W. B. Einstein and R. D. G. Jones, *Inorg. Chem.*, **11**, 395 (1972).
- (6) J. L. Hoard "Porphyrins and Metalloporphyrins", K. M. Smith, Ed., Elsevier, Amsterdam, 1975, Chapter 8.
- (7) Signs of deviations of C(n3B) and C(n4B), $n = 1, \dots, 4$, from the plane through N(1), N(2), N(3), and N(4). In all cases the C(n3)-C(n3A)-C(n3B) and C(n4)-C(n4A)-C(n4B) planes are within 8° of perpendicular to the least-squares plane defined by the atoms of the corresponding five-membered ring.
- (8) J. W. Lauber and J. A. Ibers, *J. Am. Chem. Soc.*, **95**, 5148 (1973).
- (9) Triclinic [Ni(OEP)], D. L. Cullen and E. F. Meyer, Jr., *J. Am. Chem. Soc.*, **96**, 2095 (1974); [Co(OEP)(3-Me-py)] (Me = methyl, py = pyridine), R. G. Little and J. A. Ibers, *ibid.*, **96**, 4440 (1974); [Rh(OEP)(CH₃)], A. Takenaka, S. K. Syal, Y. Sasada, T. Omura, H. Ogoshi, and Z. Yoshida, *Acta Crystallogr., Sect. B*, **32**, 62 (1976); [Sn(OEP)(Cl)₂], D. L. Cullen and E. F. Meyer, Jr., *ibid.*, **29**, 2507 (1973); [(Rh-

- (CO)₂(OEP)], A. Takenaka, Y. Sasada, H. Ogoshi, T. Omura, and Z. Yoshida, *ibid.*, **31**, 1 (1975); [(H₄OEP)²⁺(Rh(CO)₂Cl₂)₂], E. Cetinkaya, A. W. Johnson, M. F. Lappert, G. M. McLaughlin, and K. W. Muir, *J. Chem. Soc., Dalton Trans.*, 1236 (1974).
- (10) (a) ++, ++, ++, ++ for H₂(N-carboxymethyl-OEP)⁺, G. M. McLaughlin, *J. Chem. Soc., Perkin Trans.* **2**, 136 (1974); H₃(OEP)⁺, N. Hirayama, A. Takenaka, Y. Sasada, E. Watanabe, H. Ogoshi, and Z. Yoshida, *J. Chem. Soc., Chem. Commun.*, 330 (1974); [Ti(5,15-Me₂-5,15-H₂-OEP)(O)], P. N. Dwyer, L. Puppe, J. W. Buchler, and W. R. Scheidt, *Inorg. Chem.*, **14**, 1782 (1975); (H₃OEP)⁺[Re₂Cl₃(CO)₆]⁻, C. P. Hruning, M. Tsutsui, D. L. Cullen, and E. F. Meyer, Jr., *J. Am. Chem. Soc.*, **98**, 7878 (1976). (b) ++, ++, ++, ++, +- for [Co(N-(ethyl acetate)-OEP)(Cl)], D. E. Goldberg and K. M. Thomas, *ibid.*, **98**, 913 (1976). (c) ++, ++, +, - for [Co(OEP)(1-Me-Im)] (Im = imidazole), R. G. Little and J. A. Ibers, *J. Am. Chem. Soc.*, **96**, 4452 (1974). (d) ++, +, - for [Ni(5,15-Me₂-5,15-H₂-OEP)], P. N. Dwyer, J. W. Buchler, and W. R. Scheidt, *ibid.*, **96**, 2789 (1974). (e) ++, +, - for [Fe(OEP)(Im)₂], A. Takenaka, Y. Sasada, E. Watanabe, H. Ogoshi, and Z. Yoshida, *Chem. Lett.*, 1235 (1972). (f) ++, +, - for [Ru(OEP)(py)₂], F. R. Hopf, T. P. O'Brien, W. R. Scheidt, and D. G. Whitten, *J. Am. Chem. Soc.*, **97**, 277 (1975). (g) ++, - for tetragonal [Ni(OEP)], E. F. Meyer, Jr., *Acta Crystallogr., Sect. B*, **28**, 2162 (1972).
- (11) D. M. Collins, R. Countryman, and J. L. Hoard, *J. Am. Chem. Soc.*, **94**, 2066 (1972).
- (12) R. G. Little, K. R. Dymock, and J. A. Ibers, *J. Am. Chem. Soc.*, **97**, 4532 (1975).
- (13) J. R. Sams, personal communication.

Contribution from the Department of Chemistry, University of Wisconsin, Madison, Wisconsin 53706

Synthesis, X-ray Crystal Structure, and Temperature-Dependent NMR Spectrum of Tetraethylammonium (α -Methoxybenzyl)pentacarbonyl tungstate

CHARLES P. CASEY,* STANLEY W. POLICHNOWSKI, HENDRIK E. TUINSTRAS, LOREN D. ALBIN, and JOSEPH C. CALABRESE

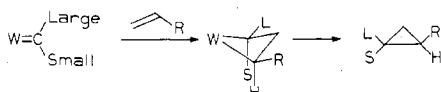
Received May 4, 1978

The reaction of (CO)₅WC(OCH₃)C₆H₅ with K⁺HB[OCH(CH₃)₂]₃⁻ followed by cation exchange with N(CH₂CH₃)₄⁺Br⁻ gives N(CH₂CH₃)₄⁺(CO)₅WCH(OCH₃)C₆H₅⁻, **3**, which is the precursor of (CO)₅WCHC₆H₅. **3** was characterized spectrally and by single-crystal X-ray diffraction. **3** crystallizes in the monoclinic system, space group P2₁/c. The unit cell constants are *a* = 12.908 (6) Å, *b* = 11.663 (6) Å, *c* = 16.875 (9) Å, β = 111.60 (4)°, and *Z* = 4. The final discrepancy indices are *R*₁ = 3.55% and *R*₂ = 4.31% for the 2941 independent reflections having *I* ≥ 2σ(*I*) in the range 3° ≤ 2θ ≤ 45°. The temperature-dependent NMR of the closely related compound N(CH₂CH₃)₄⁺(CO)₅WCH(OCH₃)C₆H₅-3,5-(CH₃)₂⁻, **5**, indicates that there is a barrier to rotation (Δ*G*[‡] = 8.7 kcal) about the aryl-benzylic carbon bond of **5**.

Introduction

(CO)₅WC(C₆H₅)₂ reacts with alkenes to give cyclopropanes, olefin scission products, and new carbene complexes.¹ A mechanistic scheme involving the equilibrium between a metallacyclobutane and a metal complex bearing both an alkene and a carbene ligand was proposed to explain these results. Earlier, a similar equilibration had been suggested by Herrisson and Chauvin² as a sufficient mechanism for the olefin metathesis reaction.³ The recent demonstration that the olefin metathesis reaction proceeds via a nonpairwise exchange of alkylidene groups is consistent with the equilibration between a metallacyclobutane and a metal complex bearing both carbene and alkene ligands and excludes mechanisms requiring the pairwise exchange of alkylidene groups of a pair of alkenes complexed to a metal.⁴

Earlier we pointed out that the moderate stereospecificity observed in the metathesis of 2-pentenes⁵ can be explained in terms of the formation of the more stable puckered metallacyclobutane in which repulsive, 1,3-diaxial interactions are minimized.^{6,7} In addition, the puckered metallacyclobutane hypothesis predicts the preferential formation of cis cyclopropanes from the reaction of a "large-small" carbene complex with a 1-alkene.⁶



Our initial attempts to test the puckered metallacyclobutane hypothesis were frustrated by the rapid decomposition of (CO)₅WC(C₆H₅)CH₃ via facile β-hydride elimination from the methyl group.⁶ In another attempt to test the puckered metallacyclobutane hypothesis, we set out to prepare

(CO)₅WC(C₆H₅)H, **1**, which could not undergo decomposition by β-hydride elimination. A two-step synthesis of **1** from (CO)₅WC(OCH₃)C₆H₅, **2**, was developed. Reduction of **2** with K⁺HB[OCH(CH₃)₂]₃⁻ gave the key intermediate N(CH₂CH₃)₄⁺(CO)₅WCH(OCH₃)C₆H₅⁻, **3**.⁸ Protonation of **3** with CF₃CO₂H at -78 °C gave the desired phenylcarbene complex **1** which was observed by ¹H NMR at -78 °C but which decomposes rapidly at -50 °C.⁸ The reactions of **1** with alkenes to give cyclopropanes will be the subject of a future paper. In this paper, we report the synthesis, X-ray crystal structure, and temperature-dependent NMR spectrum of the key intermediate, N(CH₂CH₃)₄⁺(CO)₅WCH(OCH₃)C₆H₅⁻, **3**. These findings represent the first data available on the bonding and conformational preferences in alkylpentacarbonyl tungsten compounds.

Results and Discussion

Synthesis. Since nucleophiles attack metal carbene complexes at the carbene carbon atom, we set out to prepare (CO)₅WCH(OCH₃)C₆H₅⁻ by hydride addition to aryl-methoxycarbene complexes. Addition of potassium triisopropoxyborohydride,⁹ **4**, to a red solution of (CO)₅WC(OCH₃)C₆H₅, **2**, in THF at 0 °C gave a light yellow solution. Addition of aqueous tetraethylammonium bromide followed by evaporation of THF gave an 86% yield of N(CH₂CH₃)₄⁺(CO)₅WCH(OCH₃)C₆H₅⁻, **3**, as a bright yellow solid which was further purified by recrystallization from CH₂Cl₂ at -20 °C. This reduction could also be accomplished with Na⁺HB(OCH₃)₃⁻¹⁰ but this proved to be less convenient since the later reagent decomposed at a moderate rate even when stored at -20 °C. Reduction of (CO)₅WC(OCH₃)C₆H₅ with NaBH₄ was briefly investigated by NMR; the production of (CO)₅WCH₂C₆H₅⁻¹¹ and of (CO)₅WHW(CO)₅⁻ was